Resolving photon number states in a superconducting circuit

D. I. Schuster*,[1] A. A. Houck*,[1] J. A. Schreier,[1] A. Wallraff,[1,2] J. M. Gambetta,[1]
A. Blais,[1,3] L. Frunzio,[1] B. Johnson,[1] M. H. Devoret,[1] S. M. Girvin,[1] and R. J. Schoelkopf[1]

[1]*Departments of Applied Physics and Physics, Yale University, New Haven, CT 06520*
[2]*Department of Physics, ETH Zurich, CH-8093 Zürich, Switzerland*
[3]*Département de Physique et Regroupement Québécois sur les Matériaux de Pointe, Université de Sherbrooke, Sherbrooke, Québec, Canada, J1K 2R1*

(Dated: August 30, 2006)

Electromagnetic signals are always composed of photons, though in the circuit domain those signals are carried as voltages and currents on wires, and the discreteness of the photon's energy is usually not evident. However, by coupling a superconducting qubit to signals on a microwave transmission line, it is possible to construct an integrated circuit where the presence or absence of even a single photon can have a dramatic effect. This system[2] is called circuit quantum electrodynamics (QED) because it is the circuit equivalent of the atom-photon interaction in cavity QED. Previously, circuit QED devices were shown to reach the resonant strong coupling regime, where a single qubit can absorb and re-emit a single photon many times[27]. Here, we report a circuit QED experiment which achieves the strong dispersive limit, a new regime of cavity QED in which a single photon has a large effect on the qubit or atom without ever being absorbed. The hallmark of this strong dispersive regime is that the qubit transition can be resolved into a separate spectral line for each photon number state of the microwave field. The strength of each line is a measure of the probability to find the corresponding photon number in the cavity. This effect has been used to distinguish between coherent and thermal fields and could be used to create a photon statistics analyzer. Since no photons are absorbed by this process, one should be able to generate non-classical states of light by measurement and perform qubit-photon conditional logic, the basis of a logic bus for a quantum computer.

Cavity QED[15] is a test-bed system for quantum optics[28] that allows investigations into fundamental questions on quantum measurement and decoherence, and enables applications such as squeezed light sources and quantum logic gates. To achieve this, an atom is placed between two mirrors, forming a cavity that confines the electromagnetic field and enhances the atom-photon interaction strength. Cavity QED can be characterized by this interaction strength, g, and the atom-cavity detuning, Δ, resulting in several regimes which we represent with the phase diagram in Figure 1. Resonance occurs when the detuning is less than the interaction strength ($\Delta < g$, blue region in Fig. 1), allowing real excitations to be exchanged between the atom and cavity, resulting in phenomena such as enhanced spontaneous emission into the cavity mode (the Purcell effect[20]). The *resonant strong* coupling regime of cavity QED is achieved when the coupling rate, g, is larger than the inverse atom transit time through the cavity, $1/T$, and the decay rates of the atom, γ, and cavity, κ. In this regime the photon and atom are coherently coupled, and a single photon is periodically absorbed and re-emitted (the vacuum Rabi oscillations) at a rate $2g$. Strong coupling has traditionally been studied in atomic systems using alkali atoms[25], Rydberg atoms[21], or ions[13, 14]. More recently strong coupling with solid state systems has been achieved with superconducting circuits[8, 12, 27] and approached in semiconducting quantum dots[22, 29]. The resonant strong regime of cavity QED is interesting because the joint system becomes anharmonic, allowing experiments in non-linear optics and quantum information at the single photon level.

In the dispersive (off-resonant) limit, the atom-cavity detuning is larger than the coupling, $\Delta \gg g$ and only virtual photon exchange is allowed, keeping the atom and photon largely separable (red and white regions in Fig. 1). The atom (photon) now acquires only a small photonic (atomic) component of magnitude $(g/\Delta)^2$, and an accompanying frequency shift, $2\chi = 2g^2/\Delta$. In this case the system is described to second order in g/Δ by the quantum version of the AC Stark Hamiltonian[2]:

$$H = \hbar\omega_{\rm r}\left(a^\dagger a + 1/2\right) + \hbar\omega_{\rm a}\,\sigma_{\rm z}/2 + \hbar\chi\left(a^\dagger a + 1/2\right)\sigma_{\rm z}$$

The first two terms describe a single photon mode as a harmonic oscillator and an atom or qubit as a two-level pseudo-spin system. The third term is a dispersive interaction that can be viewed as either an atom state-dependent shift of the cavity frequency or a photon number-dependent light shift (the Stark plus Lamb shifts) of the atom transition frequency. This interaction means that when the atom state is changed, an energy $2\hbar\chi$ is added or removed to or from each cavity photon. This interaction is of particular interest because it commutes with the individual atom and photon terms, meaning that it is possible to do a quantum

*Authors with contributed equally to this work.

non-demolition[7, 10] (QND) measurement of either the atom state by measuring the phase shift of photons in the cavity[26] or photon number using the atomic Stark shift[5, 23]. The demolition of a measurement is quantified by the probability that in the absence of any other decay mechanism, a repetition of the measurement will yield a different result. To realize a QND measurement, one could drive the atom at the Stark shifted atom frequency $(\omega_a + 2n\chi)$, selectively exciting it if there are exactly n photons in the cavity, and then measure the atom state independently to readout the result. In our experiment, the cavity transmission is used to measure the atom state, so while the interaction is QND, the detection performed here is not. A more fundamental limitation for any cavity QED experiment arises from the second order mixture of the atomic and photonic states, creating a probability, $(g/\Delta)^2$, that a measurement of photon number will absorb a photon or a measurement of the atomic state will induce a transition, demolishing the measured state.

In analogy with the strong resonant case, the *strong dispersive* limit can be entered when the Stark shift per photon is much larger than the decoherence rates $(2\chi > \gamma, \kappa, 1/T$ white region in Fig. 1), while the demolition remains small $(g/\Delta)^2 \ll 1$. The small number-dependent frequency shift present in the weak dispersive regime (red region Fig. 1), becomes so large that each photon number produces a resolvable peak in the atomic transition spectrum, allowing the measurement in this paper. It has been proposed that the dispersive photon shift could be used to make a QND measurement of the photon number state of the cavity using Rydberg atoms[4]. Previously attainable interaction strengths required photon number detection experiments to employ absorptive quantum Rabi oscillations in the resonant regime[6], allowing a QND measurement[17] restricted to distinguishing only between zero and one photon. More recently, a non-resonant Rydberg atom experiment entered the strong dispersive limit, measuring the single photon Wigner function with demolition $(g/\Delta)^2 = 6\%$, in principle allowing ~ 15 repeated measurements[1]. We present here a circuit QED experiment clearly demonstrating the strong dispersive regime, resolving states of up to ten photons, and having demolition $(g/\Delta)^2 < 1\%$, which should allow up to ~ 100 repeated QND measurements.

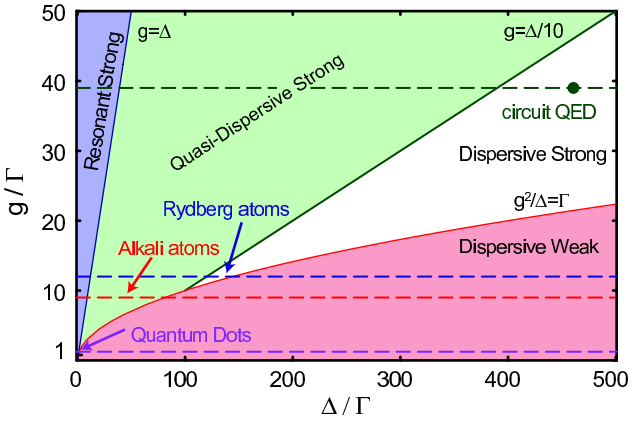

FIG. 1: A phase diagram for cavity QED. The parameter space is described by the atom-photon coupling strength, g, and the detuning Δ between the atom and cavity frequencies, normalized to the rates of decay represented by $\Gamma = \max[\gamma, \kappa, 1/T]$. Different cavity QED systems, including Rydberg atoms, alkali atoms, quantum dots, and circuit QED, are represented by dashed horizontal lines. The green circle represents the parameters used in this work. In the blue region the qubit and cavity are resonant, and undergo vacuum Rabi oscillations. In the red, weak dispersive, region the ac Stark shift $g^2/\Delta < \Gamma$ is too small to dispersively resolve individual photons, but a QND measurement of the qubit can still be realized by using many photons. In the white region, quantum non-demolition measurements are in principle possible with demolition less than 1%, allowing 100 repeated measurements. In the green region single photon resolution is possible but measurements of either the qubit or cavity occupation cause larger demolition.

In circuit QED[2, 26] the "atom"-photon interaction is implemented by a Cooper Pair Box (CPB)[3], chosen for its large dipole moment, capacitively coupled to a full-wave one-dimensional transmission line resonator. The resonator's reduced transverse dimensions, microns instead of centimeters (Fig. 2), enhance the energy density a million times over a three-dimensional microwave cavity. This large energy density, together with the large geometric capacitance (dipole moment) of the CPB, yield an interaction strength that is $g/\omega_{a,r} = 2\%$ of the total photon energy. This coupling, ten-thousand times larger than currently attainable in atomic systems, allows circuit QED to overcome the larger decoherence rates present in the solid-state environment, maintaining $g/\gamma_{\rm eff} = 40$ possible coherent vacuum Rabi oscillations in the strong resonant regime, where $\gamma_{\rm eff} = (\gamma + \kappa)/2$. The equivalent comparison of the dispersive interaction to decoherence examines the Stark shift per photon in relation to the qubit decay, $2\chi/\gamma = 6$, and determines the resolution of photon number peaks. Comparing instead to the cavity lifetime yields an estimate of the maximum number of peaks that could possibly be resolved, $2\chi/\kappa = 70$, and determines the contrast of a qubit measurement by the cavity. These values of our parameters place the system well into the strong dispersive regime.

The photon number dependent frequency shift of the qubit is detected by performing spectroscopy on the qubit-cavity system (Fig. 2e). Photons are placed in the cavity by applying a microwave signal (the cavity tone) at frequency $(\omega_{\rm rf})$ near the cavity resonance (Fig. 2e). A spectrum is taken by sweeping the frequency (ω_s) of a second microwave signal (the spectroscopy tone), which probes the qubit absorption, without significantly populating the resonator as it is detuned by many linewidths

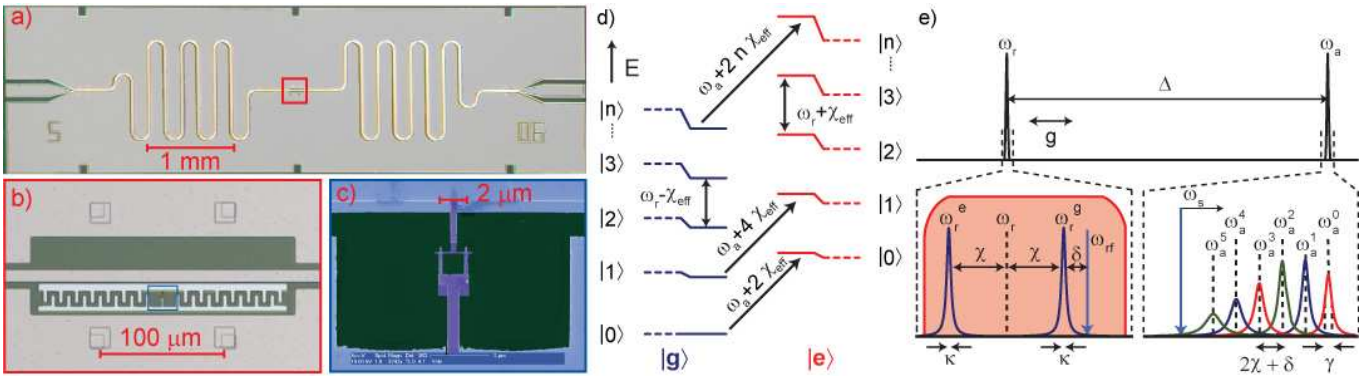

FIG. 2: Cooper Pair Box (CPB) inside cavity and spectral features of the circuit QED system. **a.** An on-chip coplanar waveguide cavity with resonant frequency $\omega_r/2\pi = 5.7\,\mathrm{GHz}$. **b.** The CPB, placed at a voltage anti-node of the coplanar waveguide (CPW) cavity (metal is beige, substrate is dark), consists of two large superconducting islands (light blue) connected by a pair of Josephson tunnel junctions (purple in **c**). Both the CPB and cavity are made from Aluminum, a superconductor at the experiment temperature, $T = 20\,\mathrm{mK}$. The transition frequency between the lowest two CPB levels is $\omega_a/2\pi \approx \sqrt{8E_J E_C}/h = 6.9\,\mathrm{GHz}$, where the Josephson energy $E_J/h = 11.5\,\mathrm{GHz}$ and the charging energy $E_C/h = e^2/2C_\Sigma h = 520\,\mathrm{MHz}$. Both the large dipole coupling, $g/2\pi = 105\,\mathrm{MHz}$, that allows access to the strong dispersive regime, and the small charging energy are due to the large geometric capacitance of the box islands to the resonator. With these parameters the transition frequency from ground to first excited state is larger by 10% than the next lowest transition, allowing the two levels to be addressed uniquely, though higher levels do contribute dispersive shifts. Most notably the nearest level causes a negative effective Stark shift per photon, $2\chi_{\mathrm{eff}} = -17\,\mathrm{MHz}$, as well as a Lamb shift-like dressing of the resonator and qubit frequencies. This dispersive shift is larger than the linewidths of both the qubit ($\gamma/2\pi = 1.9\,\mathrm{MHz}$) and cavity ($\kappa/2\pi = 250\,\mathrm{kHz}$). **d.** Dispersive cavity-qubit energy levels. Each energy level in the qubit-cavity Hamiltonian is labeled by the qubit state, where right is excited $|e\rangle$, and left is ground, $|g\rangle$, while $|n\rangle$, denotes the number of photons in the cavity. The dashed portion represents the qubit/cavity energy levels with no interaction ($g = 0$), where the solid lines show the eigenstates as they are dressed by the dispersive interaction. Transitions from $|n\rangle \rightarrow |n+1\rangle$ show the qubit-dependent cavity shift. Transitions at constant photon number from $|g\rangle\,|n\rangle \rightarrow |e\rangle\,|n\rangle$ (left to right) show a photon number dependent frequency shift $2n\chi_{\mathrm{eff}}$. **e.** Each transition in **d** can be measured in the cavity-qubit spectral response. The qubit state-dependent spectral response of the cavity is shown in the bottom left. To measure the qubit state, and also to populate the cavity in Figs. 3 and 4a-b, the cavity is driven with a coherent tone at ω_{rf}, that is blue detuned from the cavity by several linewidths to not induce any cavity nonlinearity. To attain a thermal distribution the cavity was driven with gaussian noise spanning the cavity according to the red envelope. The qubit spectrum is shown at the bottom right, and is detuned from the cavity by $\Delta/2\pi = 1.2\,\mathrm{GHz} \gg g/2\pi$. Measurements are performed by measuring qubit response to being driven with a spectroscopy tone, ω_s, by monitoring transmission at ω_{rf}. Because $\chi > \gamma$ each photon shifts the qubit transition by more than a linewidth giving a distinct peak for each number of photons in the cavity. The maximum number of resolvable peaks is determined by $2\chi/\kappa$.

$(\omega_s - \omega_r \gg \kappa)$. The detection is completed by exploiting the dual nature of the qubit-photon coupling, reusing the cavity photons as a measure of cavity transmission, demonstrated previously[2, 23, 26, 27] to measure the qubit excited state population. The measured transmission amplitude (Figs. 3-4) is an approximate measure of the actual qubit population, which could in principle be measured independently. For clarity the transmission amplitude in Figures 3-4 is plotted from high to low frequency. In order to reduce non-linearities in the response, the cavity tone was applied at a small detuning from the resonator frequency when the qubit is in the ground state $\delta/2\pi = (\omega_{\mathrm{rf}} - \omega_r^g)/2\pi = 2\,\mathrm{MHz}$ which also slightly modifies the peak splitting[9] (Fig. 2e).

The measured spectra reveal the quantized nature of the cavity field, containing a separate peak for each photon number state (Fig. 3)[9, 11]. These peaks approximately represent the weight of each Fock state in a coherent field with mean photon number $\overline{n}$, which is varied from zero to seventeen photons. At the lowest photon powers, nearly all of the weight is in the first peak, corresponding to no photons in the cavity, and confirming that the background cavity occupancy is $n_{\mathrm{th}} < 0.1$. As the input power is increased, more photon number peaks can be resolved and the mean of the distribution shifts proportional to $\overline{n}$. The data agree well with numerical solutions at low powers (solid lines in Fig. 3) to the Markovian Master equation[9, 28] with three damping sources, namely the loss of photons at rate $\kappa/2\pi = 250\,\mathrm{kHz}$, energy relaxation in the qubit at rate $\gamma_1/2\pi = 1.8\,\mathrm{MHz}$ and the qubit dephasing rate $\gamma_\phi/2\pi = 1.0\,\mathrm{MHz}$. However adequate numerical modeling of this strongly coupled system at higher photon numbers is quite difficult and has not yet been achieved.

In earlier work[5, 23] in the weak dispersive limit $(\chi/\gamma < 1)$, the measured linewidth resulted from an ensemble of Stark shifts blurring the transition, while here in the strong limit $(\chi/\gamma > 1)$ each member of the ensem-

ble is individually resolved. In the spectra measured here (Fig. 3), the linewidth of a single peak can be much less than the frequency spread of the ensemble, but changes in photon number during a single measurement can still completely dephase the qubit. Taking this into account yields a predicted photon number dependent linewidth, $\gamma_n = \gamma/2 + \gamma_\phi + (\overline{n} + n)\,\kappa/2$ for the n^{th} peak[9]. The lowest power peak (in the $\overline{n} = 0.02$ trace) corresponds to zero photons and measures the unbroadened linewidth, $\gamma_0/2\pi = 1.9\,\mathrm{MHz}$. When $\overline{n} = 2\chi_{\mathrm{eff}}/\kappa$ the peaks should begin to overlap once more, returning the system to the classical field regime. If this effect were the only limitation, we might hope to count as many as 70 photon number peaks before they merge. In practice the higher number peaks are also more sensitive to charge fluctuations in the Cooper pair box, which limits us to about 10 resolvable photon states in this measurement.

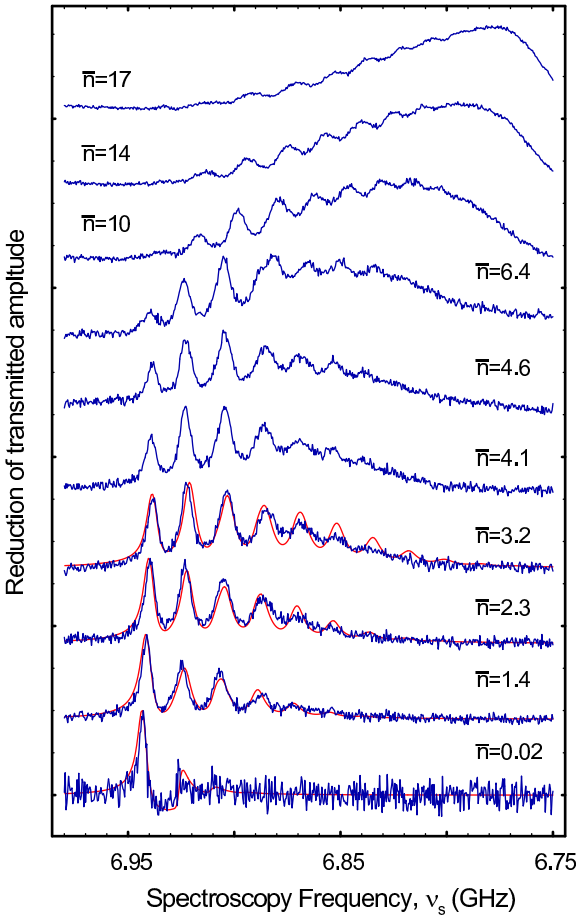

FIG. 3: Direct spectroscopic observation of quantized cavity photon number. Qubit spectra with coherent cavity drive at different average cavity occupations ($\overline{n}$). The spectra have resolved peaks corresponding to each photon number. The peaks are separated by $2\chi_{\mathrm{eff}}/2\pi = -17\,\mathrm{MHz}$. Approximately ten peaks are distinguishable. The data (blue) is well described by numerical simulations (red) with all parameters predetermined except for a single frequency offset, overall power scaling, and background thermal photon number ($n_{\mathrm{th}} = 0.1$) used for all traces. Computational limitations prevented simulations of photon numbers beyond ≈ 3. At the lowest power nearly all of the weight is in the $|0\rangle$ peak, meaning that the cavity has a background occupation less than ($n_{\mathrm{th}} < 0.1$). Peaks broaden as $(n + \overline{n})\,\kappa$ plus some additional contributions due to charge noise. At higher powers the peaks blend together and the envelope approaches a gaussian shape for a coherent state. Since $\chi < 0$, spectra are displayed from high to low frequency, and also have been normalized and offset for clarity.

The relative area under each peak in the transmission amplitude (Fig. 4) contains information about the photon statistics of the cavity field. We can compare two cases having the same average cavity occupation ($\overline{n} \sim 3$), but containing either a coherent field (Fig. 4a) or a thermal field (Fig. 4b). To create the thermal field, gaussian noise was added in a wide band around the cavity (red in Fig. 2e). The coherent and thermal states are clearly distinguishable, with the weights of the peaks being non-monotonic for a coherent distribution while the thermal distributions were monotonically decreasing for all noise intensities measured. However for the sample parame-

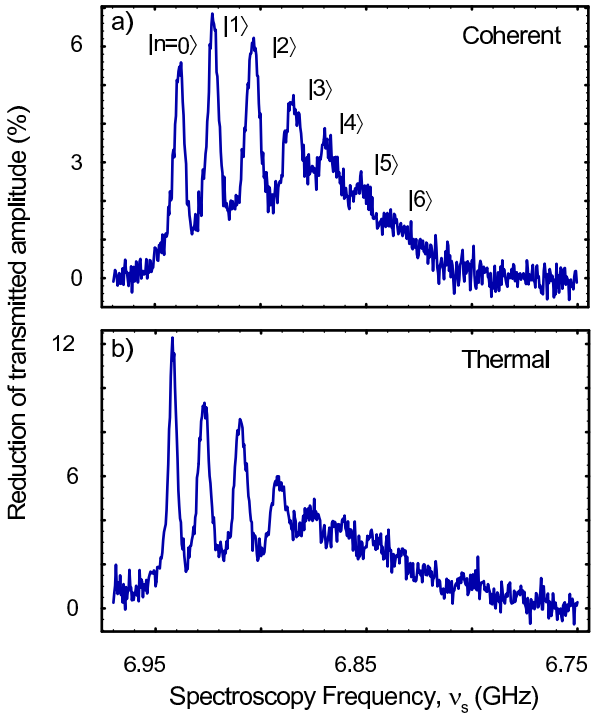

FIG. 4: Qubit spectrum distinguishes between coherent and thermal distributions. **a.** Reduction in transmitted amplitude is plotted as a proxy for qubit absorption for the case of a coherent drive with $\overline{n} = 3$ photons. **b.** Spectrum when cavity is driven with Gaussian white noise approximating a thermal state also with $\overline{n} = 3$. The coherent spectrum is clearly non-monotonic and qualitatively consistent with the Poisson distribution, $P(n) = e^{-\overline{n}}\overline{n}^n/n!$, while the thermal spectrum monotonically decreases consistent with the Bose-Einstein distribution $P(n) = \overline{n}^n/(\overline{n}+1)^{n+1}$.

ters and measurement protocols used here, several effects prevent quantitative extraction of photon number probabilities from the data. First the inhomogeneous broadening of the higher number peaks due to charge noise prevents independent extraction of their areas. Additionally, though it has been analytically shown that in the qubit absorption spectrum should accurately represent the cavity photon statistics[9], this experiment did not have an independent means to measure the qubit, and there are imperfections in mapping the qubit spectrum onto the cavity transmission. Finally, numerical simulations show that spectroscopic driving of the qubit results in complex dynamics which squeezes the cavity photon number, pointing to a path to create exotic states of light, but also obscuring the initial photon statistics. The measured data is consistent with numerical predictions which do take into account such squeezing effects (see Fig. 3) for photon numbers ($\overline{n} \leq 3$) which we could simulate. While these effects are large in the present experiment, an independent measurement of the qubit could be introduced using a second cavity or Josephson-bifurcation amplifier[24], allowing the realization of a quantitative photon statistics analyzer. Previous experiments have also measured analogous statistics of other Bosonic systems including phonons in an ion trap[13, 14], excitations in a single electron cyclotron oscillator[19], and the number of atoms in a Bose-Einstein condensate passing through a cavity[18].

The results obtained here also suggest a method for photon-qubit conditional logic. The qubit response is now strongly dependent on the number of photons in the cavity. For example, a controlled-not (CNOT) gate between a photon and qubit could be implemented by applying a π control pulse at the frequency corresponding to one photon in the cavity. This would flip the qubit if there were exactly one photon in the cavity, but do nothing for all other number states. Since the qubit does not absorb the cavity photon, the number is unchanged after the operation and could be used to entangle with distant qubits. A photon number based gate is analogous to the phonon common mode coupling used in ion-traps[16], but since the photons travel along transmission lines and not through qubits themselves, many qubits can be placed in a single wavelength, and the photons could be sent to distant qubits, including those in other cavities.

The observation of resolved photon number peaks in the qubit spectrum demonstrates a new regime for cavity QED systems, the strong dispersive limit. Measurement of the spectrum directly reveals the discrete nature of the microwave field inside the on-chip cavity. The qubit spectrum is used to distinguish field states with different photon statistics. Further exploitation of this exceptionally large vacuum Rabi coupling should enable quantum computing using transmission line cavities as a quantum bus, and allow preparation of quantum states of light for use in quantum communication and non-linear optics.

[1] P. Bertet, A. Auffeves, P. Maioli, S. Osnaghi, T. Meunier, M. Brune, J. M. Raimond, and S. Haroche. Direct measurement of the Wigner function of a one-photon Fock state in a cavity. *Physical Review Letters*, 89(20):200402, November 2002.

[2] A. Blais, R.S. Huang, A. Wallraff, S. Girvin, and R. J. Schoelkopf. Cavity quantum electrodynamics for superconducting electrical circuits: an architecture for quantum computation. *Physical Review A*, 69:062320, 2004.

[3] V. Bouchiat, D. Vion, P. Joyez, D. Esteve, and M. H. Devoret. Quantum coherence with a single Cooper pair. *Physica Scripta*, T76:165–170, 1998.

[4] M. Brune, S. Haroche, V. Lefevre, J. M. Raimond, and N. Zagury. Quantum nondemolition measurement of small photon numbers by Rydberg-atom phase-sensitive detection. *Physical Review Letters*, 65(8):976–979, August 1990.

[5] M. Brune, P. Nussenzveig, F. Schmidtkaler, F. Bernardot, A. Maali, J. M. Raimond, and S. Haroche. From Lamb shift to light shifts: vacuum and subphoton cavity fields measured by atomic phase-sensitive detection. *Physical Review Letters*, 72(21):3339–3342, May 1994.

[6] M. Brune, F. SchmidtKaler, A. Maali, J. Dreyer, E. Hagley, J. M. Raimond, and S. Haroche. Quantum Rabi oscillation: A direct test of field quantization in a cavity. *Physical Review Letters*, 76(11):1800–1803, March 1996.

[7] C. M. Caves, K. S. Thorne, R. W. P. Drever, V. D. Sandberg, and M. Zimmermann. On the measurement of a weak classical force coupled to a quantum-mechanical oscillator. *Reviews of Modern Physics*, 52(2):341–392, 1980.

[8] I. Chiorescu, P. Bertet, K. Semba, Y. Nakamura, C. J. Harmans, and J. E. Mooij. Coherent dynamics of a flux qubit coupled to a harmonic oscillator. *Nature*, 431(7005):159–162, September 2004.

[9] J. Gambetta, Blais A., Schuster D. I., A. Wallraff, L. Frunzio, J. Majer, S. M. Girvin, and R. J. Schoelkopf. Qubit-photon interactions in a cavity: Measurement induced dephasing and number splitting. *Submitted to Physical Review A*, 2006.

[10] P. Grangier, J. A. Levenson, and J. P. Poizat. Quantum non-demolition measurements in optics. *Nature*, 396(6711):537–542, December 1998.

[11] E. K. Irish and K. Schwab. Quantum measurement of a coupled nanomechanical resonator - Cooper pair box system. *Physical Review B*, 68(15):155311, October 2003.

[12] J. Johansson, S. Saito, T. Meno, H. Nakano, M. Ueda, K. Semba, and H. Takayanagi. Vacuum Rabi oscillations in a macroscopic superconducting qubit LC oscillator system. *Physical Review Letters*, 96(12):127006, March 2006.

[13] D. Leibfried, D. M. Meekhof, B. E. King, C. Monroe, W. M. Itano, and D. J. Wineland. Experimental determination of the motional quantum state of a trapped atom. *Physical Review Letters*, 77(21):4281–4285, November 1996.

[14] D. Leibfried, D. M. Meekhof, C. Monroe, B. E. King, W. M. Itano, and D. J. Wineland. Experimental preparation and measurement of quantum states of motion of a trapped atom. *Journal of Modern Optics*, 44(11-12):2485–2505, 1997.

[15] H. Mabuchi and A. C. Doherty. Cavity quantum

electrodynamics: Coherence in context. *Science*, 298(5597):1372–1377, November 2002.

[16] C. Monroe, D. M. Meekhof, B. E. King, W. M. Itano, and D. J. Wineland. Demonstration of a fundamental quantum logic gate. *Physical Review Letters*, 75(25):4714–4717, December 1995.

[17] G. Nogues, A. Rauschenbeutel, S. Osnaghi, M. Brune, J. M. Raimond, and S. Haroche. Seeing a single photon without destroying it. *Nature*, 400(6741):239–242, July 1999.

[18] A. Ottl, S. Ritter, M. Kohl, and T. Esslinger. Correlations and counting statistics of an atom laser. *Physical Review Letters*, 95(9):090404, August 2005.

[19] S. Peil and G. Gabrielse. Observing the quantum limit of an electron cyclotron: QND measurements of quantum jumps between Fock states. *Physical Review Letters*, 83(7):1287–1290, August 1999.

[20] E. M. Purcell. Spontaneous emission probabilities at radio frequencies. *Physical Review*, 69(11-1):681–681, 1946.

[21] J. M. Raimond, M. Brune, and S. Haroche. Manipulating quantum entanglement with atoms and photons in a cavity. *Reviews of Modern Physics*, 73(3):565–582, July 2001.

[22] J. P. Reithmaier, G. Sek, A. Loffler, C. Hofmann, S. Kuhn, S. Reitzenstein, L. V. Keldysh, V. D. Kulakovskii, T. L. Reinecke, and A. Forchel. Strong coupling in a single quantum dot-semiconductor microcavity system. *Nature*, 432(7014):197–200, November 2004.

[23] D. I. Schuster, A. Wallraff, A. Blais, R. S. Huang, Majer J., S. Girvin, and R. Schoelkopf. AC-Stark shift and dephasing of a superconducting qubit strongly coupled to a cavity field. *Physical Review Letters*, 94:123602, 2005.

[24] I. Siddiqi, R. Vijay, M. Metcalfe, E. Boaknin, L. Frunzio, R. J. Schoelkopf, and M. H. Devoret. Dispersive measurements of superconducting qubit coherence with a fast latching readout. *Physical Review B*, 73(5):054510, February 2006.

[25] R. J. Thompson, G. Rempe, and H. J. Kimble. Observation of normal-mode splitting for an atom in an optical cavity. *Physical Review Letters*, 68(8):1132–1135, February 1992.

[26] A. Wallraff, D. I. Schuster, A. Blais, L. Frunzio, J. Majer, S. M. Girvin, and R. J. Schoelkopf. Approaching unit visibility for control of a superconducting qubit with dispersive readout. *Physical Review Letters*, 95:060501, 2005.

[27] A. Wallraff, D. I. Schuster, A. Blais, R.-S. Huang, J. Majer, S. Kumar, S. M. Girvin, and R. Schoelkopf. Circuit quantum electrodynamics: Coherent coupling of a single photon to a Cooper pair box. *Nature*, 431:162, 2004.

[28] D. F. Walls and G. J. Milburn. *Quantum optics*. Springer, 2006.

[29] T. Yoshie, A. Scherer, J. Hendrickson, G. Khitrova, H. M. Gibbs, G. Rupper, C. Ell, O. B. Shchekin, and D. G. Deppe. Vacuum Rabi splitting with a single quantum dot in a photonic crystal nanocavity. *Nature*, 432(7014):200–203, November 2004.

This work was supported in part by the National Security Agency under the Army Research Office, the NSF, the W. M. Keck Foundation, and Yale University. A.H. would like to acknowledge support from Yale University via a Quantum Information and Mesoscopic Physics Fellowship. A.B. was supported by NSERC, CIAR and FQRNT. Numerical simulations were performed on a RQCHP cluster. The authors declare that they have no competing financial interests. Correspondence and requests for materials should be addressed to Rob Schoelkopf (email:Robert.Schoelkopf@yale.edu).